Seventh International Conference on CFD in the Minerals and Process Industries
CSIRO, Melbourne, Australia
9-11 December 2009

APPLICATION OF THE PARTICLE IN CELL APPROACH FOR THE SIMULATION OF BUBBLING FLUIDIZED BEDS OF GELDART A PARTICLES

Shayan KARIMIPOUR[1], Todd PUGSLEY[*1]

[1] Department of Chemical Engineering, University of Saskatchewan, Saskatoon, SK, S7N 5A9, Canada
*Corresponding author, E-mail address: todd.pugsley@usask.ca

ABSTRACT

Computational Fluid Dynamic (CFD) modelling of gas-solid fluidized beds has been an active area of research for several decades. Although CFD models have been able to provide acceptable predictions of the behaviour of fluidized beds containing Geldart B particles, models for Geldart A particles have been less successful. This difficulty arises due to the relative importance of interparticle cohesive forces when fluidizing Geldart A particles.

In the present work, the capability of the multiphase Particle in Cell (PIC) approach for modeling a bubbling fluidized bed of Geldart A particles has been investigated. Four different simulation cases, which include three different mesh sizes and two drag models with a realistic particle size distribution, have been designed and tested. Bubble properties have been extracted from the model predictions and compared with the predictions of empirical correlations as well as experimental data. The results show a promising predictive capability of the multiphase PIC approach without the need to modify the drag force or other constitutive relationships in the model.

NOMENCLATURE

A particle acceleration (m/s^2)
C particle velocity fluctuations averaged over the velocity space (m/s)
C_D drag coefficient
dp particle diameter (m)
D drag function (kg/m^{3}s)
D_1 drag function in drag model 2 (kg/m^{3}s)
D_2 drag function in drag model 2 (kg/m^{3}s)
F rate of momentum exchange per unit volume from the gas to the particle phase (N/m^{3}s)
g gravitational acceleration (m/s^2)
g_0 solid radial distribution function
n_p number of particles in a parcel
N_p number of parcels or clouds
p gas pressure (kPa)
Re Reynolds number
u_g gas velocity (m/s)
u_p particle velocity (m/s)
$\overline{u}_p$ mean particle velocity (m/s)
V_p particle volume (m^3)
x particle position (m)

Greek Letters
ε gas volume fraction
γ restitution coefficient
μ_g gas viscosity (kg/m s)
ρ_g gas density (kg/m^3)
$\overline{\rho}_p$ average particle density (kg/m^3)
ρ_p particle density (kg/m^3)
τ continuum particle normal stress (N/m^2)
∇_{up} Divergence operator with respect to velocity
θ particle volume fraction
θ_{cp} particle-phase volume fraction at close packing
Θ granular temperature (m^2/s^2)

INTRODUCTION

Although CFD modeling of single phase systems is now a common task, using CFD tools for modeling multiphase systems is still far from perfected. This is due in part to the difficulties encountered in describing the interactions between different phases. Systems containing one or more particulate phases are usually the most complex and challenging ones in the field of multiphase flows. The interaction between the particles themselves and the particles and gas are essential in particulate systems and should be thoroughly understood to be able to provide a comprehensive model of the process.

CFD two-fluid models, or TFM, in which the gas and solid phases are treated as two separate but fully interpenetrating continua, have been able to provide acceptable results for the simulation of coarser particles (Goldschmidt et al., 2001; Taghipour et al., 2005; Boemer et al., 1997), belonging to the Geldart B classification of powders (Geldart, 1973). However attempts at the simulation of the finer Geldart A class of powders have encountered some significant challenges (McKeen and Pugsley, 2003; Makkawi et al., 2006). This difficulty arises due to the relative importance of interparticle cohesive forces compared with gravitational forces when dealing with Geldart A powders (Massimilla and Donsi, 1976). According to Molerus (1982), the cohesion forces can be neglected for larger particles such as group B and D particles. Neglecting the cohesion forces in CFD models of dense fluidized beds of Geldart A particles leads to as much as 100% over-prediction of the bed expansion (McKeen and Pugsley, 2003; Makkawi et al., 2006). In fact, by neglecting these forces the underlying assumption is that mainly the collisional effects control individual particle-particle contacts, thus a large part of the remaining dynamic energy of the particles is consumed for propelling the particles towards the top of the bed.

McKeen and Pugsley (2003) were among the early researchers who reported this over-prediction of bed expansion. They argued that interparticle forces lead to the formation of small clusters with a corresponding reduction in gas-solid drag. They found that by scaling the drag model of Gibilaro et al. (1985) with a fractional

constant equal to 0.25, realistic bed expansion and bubble properties were predicted. Kim and Arastoopour (2002) tried to extend the kinetic theory to cohesive particles by modifying the solid distribution equation. However, the final expression for the particulate stress was complex and difficult to incorporate into the current continuous models (Kim and Arastoopour, 2002). Both their model and the model of McKeen and Pugsley (2003) did not consider the coexistence of particles with different sizes in the fluidized bed.

As indicated by Grace and Sun (1991), particle size distribution has a significant influence on the bed expansion. Therefore, it seems possible that consideration of the size distribution in the CFD models might eliminate the problem of over-prediction of the bed expansion. However, the presence of different types and sizes of particles complicates the modeling effort because separate continuity and momentum equations must be solved for each size and type (Gidaspow, 1994; Risk, 1993). As a result models have been only used for up to three solid 'phases' (*ie* three particle sizes) in the literature, due to the computational limitations. The multiphase Particle in Cell (PIC) approach (Snider, 2001; Snider et al., 1998; Andrews and O'Rourke, 1996) provides a numerical scheme in which particles are grouped into computational parcels each containing a number of particles with identical density, volume and velocity, located at a specific position. The evolution of the particle phase is governed by solving a Liouville equation for the particle distribution. The result of this procedure is a computational technique for multiphase flow that can handle a distribution of particle types and sizes. Detail of the model is provided in the next sections.

In the present work, the capability of the multiphase Particle in Cell (PIC) approach for simulating the bubbling fluidized bed of Geldart A particles is investigated. The simulation results for different parameters will be compared with published correlations for these parameters and experimental data.

MODEL DESCRIPTION

Governing Equations

In the PIC approach, the mass and momentum equations are solved for the continuous phase (fluid) and a Liouville equation is solved for the particle phase to find the distribution of particle positions with different velocities and sizes. An isotropic solids stress that depends on the particle volume fraction is then used to model the average collisional force (Gidaspow, 1986; Harris and Crighton, 1994). The mass and momentum equations for the gas phase are as follows, respectively (Gidaspow, 1994; Batchelor, 1988; Williams, 1985):

$$\frac{\partial(\varepsilon\rho_g)}{\partial t} + \nabla_x(\varepsilon\rho_g u_g) = 0 \quad (1)$$

$$\frac{\partial(\varepsilon\rho_g u_g)}{\partial t} + \nabla_x(\varepsilon\rho_g u_g u_g) = -\nabla_x p - \boldsymbol{F} + \varepsilon\rho_g g \quad (2)$$

where F is the rate of momentum exchange per unit volume between the fluid and particle phase. The detailed expression for F will be given later.

The Liouville equation is used to find the particle distribution function $f(x,\ u_p,\ \rho_p,\ V_p,\ t)$ at each time (Williams, 1985):

$$\frac{\partial f}{\partial t} + \nabla_x(f\boldsymbol{u}_p) + \nabla_{\boldsymbol{u}_p}(fA) = 0 \quad (3)$$

The Liouville equation is a differential equation which gives the future coordinates of the particles based on the current coordinates and properties of the particles in the phase space. It is assumed that the mass of each particle is constant in time (no mass transfer between particles or to the fluid), but particles can have a distribution of sizes and densities. Particles are grouped into computational parcels each containing N_p particles with identical density, volume, and velocity, located at position, x_p. The Liouville equation, Eq. (3), conserves the particle numbers in parcel volumes, V_p, moving along dynamic trajectories in particle phase space.

In Eq. (3), A is the particle acceleration, $\mathrm{d}u_p/\mathrm{d}t$, and can be calculated from the following equation:

$$A = \frac{1}{\rho_p} D(u_g - u_p) - \frac{1}{\rho_p}\nabla_x p + g - \frac{1}{\theta\rho_p}\nabla_x \tau \quad (4)$$

Drag Models

The two drag models used in this work are provided in Table 1. In Fig. 1, these two drag models are compared with other well-known drag models from the open literature that have been used by CFD modelers. The drag model number 1 used here, is the model proposed by Wen and Yu (1966) where the equation of Schiller and Naumann (1935) is used for calculating the drag coefficient of a single particle. The number 2 drag model is a modified version of Gidaspow's drag model (Gidaspow, 1994). In this model, the Ergun equation (Ergun, 1952) is used for voidages less than 0.8 and the Wen and Yu drag model (Wen and Yu, 1966) for voidages greater than 0.8. Another drag model graphed in Fig. 1 is the drag model of Syamlal and O' Brien (1989), in which the coefficients of the model are modified based on the minimum fluidization velocity using the method proposed by the authors. The drag models proposed by Gibilaro et al. (1985) and its scaled version used by McKeen and Pugsley (2003) are the other drag models compared in Fig 1. As the figure shows, to be able to predict a realistic bed expansion, McKeen and Pugsley (2003) had to scale down the Gibilaro drag model by 75%. However, both drag models used in this study are in the range of the other drag models and as will be shown later, there was no need for scaling.

Solid Stress Models

The particle normal stress model used in this study is the Lun et al. (1987) model which is developed based on the dense phase kinetic theory of gases:

$$\tau = \left[\theta\bar{\rho}_p + \theta^2\bar{\rho}_p(1+\gamma)g_0\right]\Theta \quad (5)$$

It is assumed in Eq. (5) that the acceleration of an individual particle due to the solids stress is independent of size and velocity of the particle.

The solids stress equation is comprised of two parts. The first part represents the kinetic contribution and the second part represents the collisional contribution. In a physical view, the kinetic part accounts for the momentum transferred by particles moving across imaginary shear layers in the system. The collisional part refers to the momentum transferred by direct particulate collisions.

The granular temperature, Θ, is given by

$$\Theta = \frac{1}{3}\left\langle C^2 \right\rangle \tag{6}$$

The radial distribution function can be defined as follows (Gidaspow, 1994):

$$g_0 = \frac{3}{5}\left[1 - \left(\frac{\theta}{\theta_{cp}}\right)^{1/3}\right]^{-1} \tag{7}$$

Model 1:

$$C_D = \frac{24}{Re} \qquad Re < 0.5$$

$$C_D = \frac{24}{Re}\left(1 + 0.15Re^{0.687}\right) \qquad 0.5 \le Re < 1000$$

$$C_D = 0.44 \qquad Re \ge 1000$$

$$D = \frac{3}{4} C_D \rho_g \theta \frac{\left|u_g - u_p\right|}{d_p} \varepsilon^{-1.65}$$

$$Re = \frac{\rho_g \varepsilon d_p \left|u_g - u_p\right|}{\mu_g}$$

Model 2:

$$C_D = \frac{24}{Re} \qquad Re < 0.5$$

$$C_D = \frac{24}{Re}\left(1 + 0.15Re^{0.687}\right) \qquad 0.5 \le Re < 1000$$

$$C_D = 0.44 \qquad Re \ge 1000$$

$$D_1 = \frac{3}{4} C_D \rho_g \theta \frac{\left|u_g - u_p\right|}{d_p} \varepsilon^{-1.65}$$

$$D_2 = \left(\frac{180\theta}{Re} + 2\right)\frac{\left|u_g - u_p\right|}{d_p}\rho_g \theta$$

$$Re = \frac{\rho_g \varepsilon d_p \left|u_g - u_p\right|}{\mu_g}$$

$$D = D_1 \qquad \theta < 0.75\theta_{CP}$$

$$D = \frac{\theta - 0.85\theta}{0.85\theta_{CP} - 0.75\theta_{CP}}\left(D_2 - D_1\right) + D_1 \qquad 0.75\theta_{CP} \le \theta \le 0.85\theta_{CP}$$

$$D = D_2 \qquad \theta > 0.85\theta_{CP}$$

Table 1: Equations of drag models.

In concept, the radial distribution function provides a correction to the probability of a collision due to the presence of other particles. In the case of slightly inelastic collisions, where the collisional anisotropy plays a negligible role, the radial distribution function depends only on the local particle volume fraction (Ye et al., 2005).

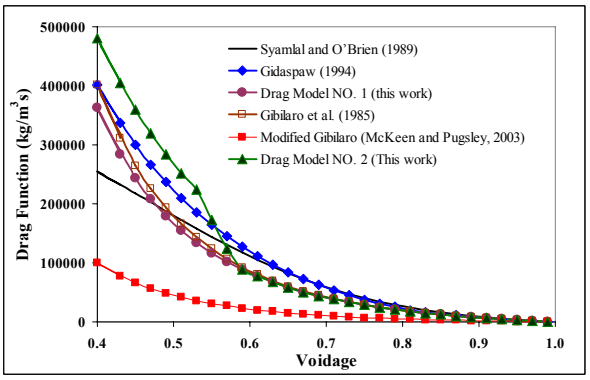

Figure 1: Comparison between different drag models used for CFD simulations in the literature.

Particle Phase

By using the Liouville equation for calculating the particle probability distribution function, Eq. (3), integrated over velocity, density and volume of all particles, the probable number of particles per unit volume at x and t that have the velocity, density and volume in the interval of (u_p, u_p+du_p), (ρp, ρ_p+dρ_p) and (V_p, V_p+dV_p) can be obtained. In this way, the size distribution of the particles is applied in calculating the interphase momentum transfer.

The particle volume fraction, θ, is defined from the particle distribution function, f, as

$$\theta = \iiint f V_p dV_p d\rho_p d\boldsymbol{u}_p \tag{8}$$

Then ε and θ are related by

$$\varepsilon + \theta = 1 \tag{9}$$

An expression for the interphase momentum transfer per unit volume between the fluid and particle phases is needed to complete the equations:

$$\boldsymbol{F} = \iiint f V_p \rho_p \left[D(\boldsymbol{u}_g - \boldsymbol{u}_p) - \frac{1}{\rho_p}\nabla p\right] dV_p d\rho d\boldsymbol{u}_p \tag{10}$$

The particle phase is implicitly coupled to the fluid phase through the interphase drag force.

Solution Procedure

Each computational parcel contains n_p real particles with identical density, ρ_p, velocity, u_p, volume, V_p, and position, x_p. The Liouville equation, Eq. (3), is the mathematical expression of conservation of particle numbers in these parcel volumes moving along dynamic trajectories in the particle phase. The number of particles n_p associated with a parcel is constant in time. The particle positions are updated using the following implicit approximations:

$$\boldsymbol{x}_p^{n+1} = \boldsymbol{x}_p^n + \boldsymbol{u}_p^{n+1}\Delta t \tag{11}$$

The particle velocity is updated by integration of Eq. (4).

$$\boldsymbol{u}_p^{n+1} = \frac{\boldsymbol{u}_p^n + \Delta t\left[D\,\boldsymbol{u}_{f,p}^{n+1} - \frac{1}{\rho_p}\nabla p_p^{n+1} - \frac{1}{\rho_p \theta_p}\nabla \tau_p^{n+1} + g\right]}{1 + \Delta t\, D} \tag{12}$$

where $\boldsymbol{u}_p^{n+1}$ is the interpolated implicit particle velocity at the particle location, p_p^{n+1} is the interpolated implicit

pressure gradient at the particle location, τ_p^{n+1} is the interpolated solids stress gradient at the particle location. The particle velocity given by Eq. (12) can be solved directly at each time step using fluid properties updated from the current time step and old-time properties for the solids stress. Following the particle velocity calculation, the particle positions are updated. The final grid volume fraction is calculated by mapping the particle volumes to the grid. This volume fraction will be used for the solution of gas continuity and momentum equations in the next time step. The new-time fluid volume fraction is calculated using the conservation of volume equation, Eq. (9).

MODEL SET UP AND PARAMETERS

Fluidized Bed and Flow Conditions

A fluidized bed with 50 cm static bed depth containing FCC (Geldart A) particles with aSauter mean diameter of 79 μm and the particle size distribution given in Fig. 2, was defined for all simulation cases. Three dimensional uniform meshes with mesh sizes of 0.5, 1, and 2 cm have been used to examine mesh dependency. The superficial gas velocity was 0.1 m/s, which is the same as that used by McKeen and Pugsley (2003) in a fluidized bed test rig of the same diameter and static bed depth and with FCC particles of the same mean diameter. The values for different parameters used in the model are provided in Table 2. The simulations in this work were carried out with the commercial CFD code BARRACUDA® from CPFD-Software Technology, Albuquerque, NM, USA.

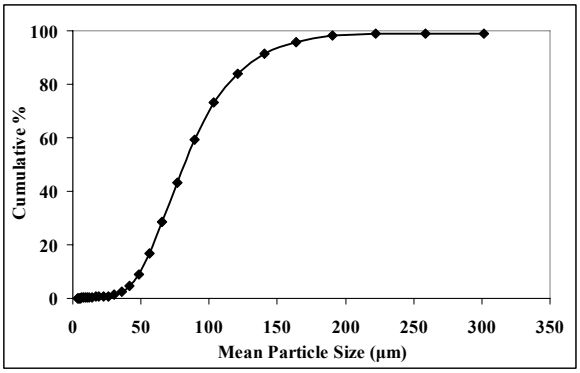

Figure 2: Cumulative particle size distribution of the FCC powders used in the experiments.

Boundary and Initial Conditions

A Dirichlet boundary condition was defined for the gas phase entering at the bottom of the fluidized bed in which the superficial gas velocity is specified. A constant pressure (atmospheric pressure) upper boundary condition was employed at the bed exit. A uniform pressure equal to the atmospheric pressure and uniform gas velocity equal to the superficial gas velocity at minimum fluidization was defined throughout the column as the initial conditions. The initial solid fraction of the bed was considered to be equal to the solid fraction at the minimum fluidization condition.

ANALYSIS AND RESULTS

The model predictions have been compared with correlations for bubble properties as well as the experimental data of McKeen and Pugsley (2003). Fig. 3 provides the cross-sectionally averaged axial profile of the solid fraction inside the fluidized bed. With the exception of the case corresponding to the 2 cm uniform mesh, both drag models predict an almost uniform axial solid fraction profile with a sudden decrease in the solid fraction. This sharp decrease corresponds to the interface of the upper surface of the dense bed and the dilute freeboard region above.

The percentage of expansion from the static bed height for all simulation cases are also given in Fig. 3. The values of bed expansion show that both drag model and mesh size are important in prediction of bed expansion and their effect are comparable. It is also observable that the capability of the model for predicting a correct bed expansion highly deteriorates with increasing the mesh size.

Geometry	Three-dimensional, Cartesian
Vessel dimension	0.14 m diameter and 1 m height
Grid	0.5*0.5*0.5, 1*1*1, 2*2*2 cm
Total number of particles	1.31472e+10
Total number of clouds	3.8944e+6
Granular viscosity model	Lun et al. (1984)
Drag model	No. 1 and No. 2 in Table 1
Flow type	Compressible with no gas-phase turbulence
Simulation time	25 seconds
Time step	0.0001 s
Pressure-Velocity coupling	SIMPLE
Maximum solid packing volume fraction	0.55
Initial condition	Bed at minimum fluidization
Minimum fluidization velocity	0.004 m/s
Minimum fluidization voidage	0.45
Boundary conditions	Uniform flow from bottom Atmospheric pressure at the top
Gas superficial velocity	0.1 m/s
Static bed depth	0.5 m
Restitution coefficient	0.4

Table 2: Input parameters used in the simulation.

The dependency of the bed expansion on the mesh size was also reported recently by Wang et al. (2009). They found that a very small time step and a highly refined mesh (of the order of three particle diameters for the case they studied) is required for correct prediction of the bed expansion using the TFM approach. Employing such small mesh sizes makes solution of the model exceedingly computer intensive and time consuming, thus decreases the model's functionality for larger scale applications. As Fig. 3 illustrates, the PIC approach is able to predict the correct value of the bed expansion without resorting to such a highly refined mesh.

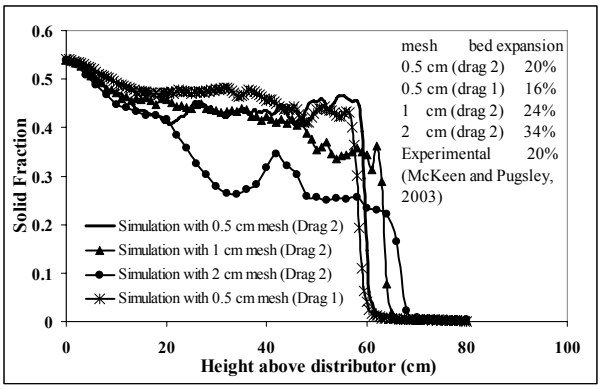

Figure 3: Cross sectional average axial profile of the solid fraction inside the fluidized bed, U_0=0.1 m/s, averaged over the period 10-25 s.

Fig. 4 provides a comparison of the average equivalent bubble diameter as a function of height above the distributor predicted by our model, with values of the bubble diameter predicted by selected empirical correlations from the literature. The simple correlation of Hilligardt and Werther (1986) and the more elaborate correlations of Horio and Nonako (1987) and Choi et al. (1998) that account for bubble coalescence and splitting have been used here.

Consistent with the copious amount of experimental evidence on the topic, the model predicts that bubble size increases with increasing height above the distributor inlet. The profile calculated for 0.5 cm mesh and different drag models produce similar predictions, which indicate negligible effect of the drag function. It is also interesting to note that the trends of the model predictions suggest a levelling-off of bubble growth as the upper surface of the bed is reached. This notion of a maximum bubble size for Geldart A powders is consistent with the trends of the correlations and also experimental evidence in the fluidization literature. As can be seen from the figure, the correlation results are generally higher than the simulation results. The difference between the results of various correlations is also noticeable. In order to make these correlations usable over a wider range of particle size, the available experimental data and correlations for different particle sizes have been employed in developing these correlations. However, most of the available data are based on Geldart B and larger particles. Therefore, since bubbles are larger for larger particles, these correlations might not be completely appropriate for predicting smaller bubbles that appear in the fluidization of Geldart A particles. This fact needs to be further investigated using the experimental data of Geldart A particles only.

Small bubbles form at the distributor and start moving upward right after formation. The size of the bubbles increases as the upper bed surface is approached. During this upward travel, the bubble velocity also increases due to increasing bubble size (Boemer et al., 1998). Fig. 5 compares the model and correlation predictions of bubble velocity with selected experimental data available in the literature for Geldart A particles. For calculating the bubble velocity, the rise velocity of a single bubble is needed. The correlation proposed by Wallis (1969) that accounts for the effect of the system geometry on the bubble rise velocity has been used for this purpose. As can be seen in the figure, the bubble velocities output by our PIC model fall within the range of the predictions of literature correlations and experimental data.

DISCUSSION

The predictions of our PIC model presented in the previous section, illustrate that, compared to the effect of the mesh size, the choice of drag model has a minor effect on the model results. As mentioned before, a key advantage of the PIC method is the consideration of the size distribution of particles in the formulation. This distribution influences the calculation of the momentum exchange term between the particulate and fluid phases. Although the drag force in both PIC and TFM models is multiplied by relative velocity between gas and solids, the distribution of particle sizes and their proper relative velocity is not considered in TFM models.

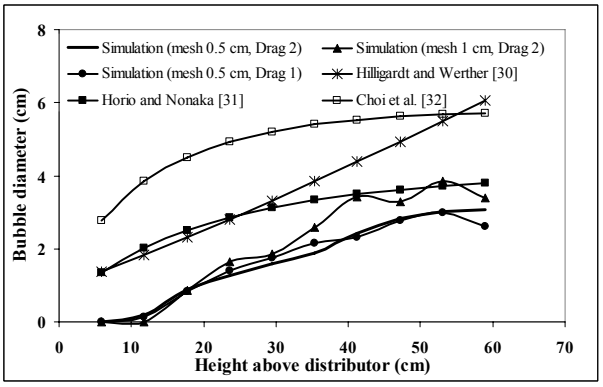

Figure 4: Comparison of the bubble average equivalent diameter as a function of height above the distributor with the available correlations.

While increasing the resolution of the numerical grid enhances the predictions of the model, computation time also dramatically increases. For instance, the time for modelling 25 s of real time using a 0.5 cm mesh is 40 days compared to 13 days for 1 cm mesh. Since the simulation case with 1 cm mesh showed the ability to provide good results in many aspects, using this coarser mesh may be a reasonable choice, especially for large simulation cases.

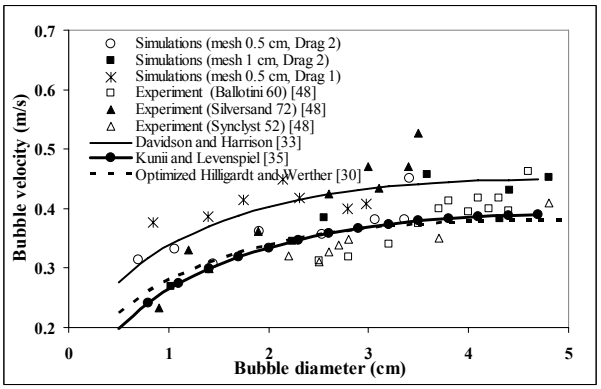

Figure 5: Comparison of the variation of the bubble velocity with bubble diameter with the available correlations and experimental data.

CONCLUSION

In the present work, the capability of the multiphase Particle in Cell (PIC) approach with a realistic particle size distribution for modeling the bubbling behaviour bed of a fluidized bed of Geldart A particles was investigated. Four cases with three different mesh sizes and two drag models were modeled. Model predictions of bubble size and bubble rise velocity as well as bed expansion were compared with commonly accepted correlations as well as experimental data from the literature. The results show a very promising prediction capability of the multiphase PIC approach without resorting to modification in the drag model. The results also indicate that although both mesh size and choice of drag model affect the predictions, the influence of the drag model is negligible compared to the effect of the mesh size.

REFERENCES

ANDREWS, M.J., O'ROURKE, P.J., (1996), "The multiphase particle-in-cell (MP-PIC) method for dense particulate flows", *Int. J. Multiphase Flow*, **22**, 379-402.

BATCHELOR, G., (1988), "A new theory of the instability of a uniform fluidized bed", *J. Fluid Mech.*, **193**, 75-110.

BOEMER, A., QI, H., RENZ, U., (1997), "Eulerian simulation of bubble formation at a jet in a two-dimensional fluidized bed", *Int. J. Multiphase Flow*, **23**, 927-944.

BOEMER, A., QI, H., RENZ, U., (1998) "Verification of Eulerian simulation of spontaneous bubble formation in a fluidized bed", *Chem. Eng. Sci.*, **53**, 1835-1846.

CHOI, J., SON, J., KIM, S., (1998), "Generalized model for bubble size and frequency in gas fluidized beds", *Ind. Eng. Chem. Res.*, **37**, 2559-2564.

DAVIDSON J., HARRISON, D., (1963), "Fluidized Particles", Cambridge University Press, New York.

ERGUN, S., (1952), "Fluid flow through packed columns", *Chem. Eng. Prog.*, **48**, 89-94.

GELDART, D., (1973), "Types of gas fluidization", *Powder Tech.*, **7**, 285-292.

GIBILARO, L., DI FELICE, R., WALDRAM, S., (1985), "Generalized friction factor and drag coefficient correlations for fluid-particle interactions", *Chem. Eng. Sci.*, **40**, 1817-1823.

GIDASPOW, D., (1994), "Multiphase flow and fluidization continuum and kinetic theory description", Academic Press, Boston.

GIDASPOW, D. (1986), "Hydrodynamics of fluidization and heat transfer: supercomputer modelling", *Appl. Mech. Rev.*, **39**, 1-22.

GOLDSCHMIDT, M., KUIPERS, J., VAN SWAAIJ, W., (2001), "Hydrodynamic modelling of dense gas-fluidised beds using the kinetic theory of granular flow: effect of coefficient of restitution on bed dynamics", *Chem. Eng. Sci.*, **56**, 571-578.

GRACE, J., SUN, G., (1991), "Influence of particle size distribution on the performance of fluidized bed reactors", *Can. J. Chem. Eng.*, **69**, 1126-1134.

HARLOW, F., AMSDEN, A., (1975), "Numerical calculation of multiphase fluid flow", *J. Comput. Phys.*, **17**, 19-52.

HARRIS, S. CRIGHTON, D., (1994), "Solutions, solitary waves and voidage disturbances in gas-fluidized beds", *J. Fluid Mech.*, **266**, 243-276.

HILLIGARDT, K., WERTHER, J., (1986), "Local bubble gas hold-up and expansion of gas-solid fluidized beds", *Ger. Chem. Eng.*, **9**, 215-221.

HORIO, M., NONAKA, A., (1987), "A generalized bubble diameter correlation for gas-solid fluidized beds", *AIChE J.*, **33**, 1865-1872.

KIM, H., ARASTOOPOUR, H., (2002), "Extension of kinetic theory to cohesive particle flow", *Powder Tech.*, **122**, 83-94.

KUNII, D. AND LEVENSPIEL, O., (1991), In: (2nd Edn. ed.), "Fluidization Engineering", Butterworth-Heinemann, Boston, MA, U.S.A.

LUN, C.K.K., SAVAGE, S.B., (1987), "A simple kinetic theory for granular flow of rough, inelastic spherical particles", *J. Fluid Mech.*, **54**, 47-53.

MAKKAWI, Y., WRIGHT, P., OCONE, R., (2006), "The effect of friction and inter-particle cohesive forces on the hydrodynamics of gas-solid flow: A comparative analysis of theoretical predictions and experiments", *Powder Tech.*, **163**, 69-79.

MASSIMILLA, L., DONSI, G., (1976), "Cohesive forces between particles of fluid-bed catalysts", *Powder Tech.*, **15**, 253-260.

MCKEEN, T., PUGSLEY, T., (2003), "Simulation and experimental validation of freely bubbling bed of FCC catalyst", *Powder Tech.*, **129**, 139-152.

MOLERUS, O., (1982), Interpretation of Geldart type A, B, C and D powders by taking into account interparticle forces", *Powder Tech.*, **33**, 81-87.

RISK, M., (1993), "Mathematical modeling of densely loaded, particle laden turbulent flows", *Atomization Sprays*, **3**, 1-27.

SCHILLER, L., NAUMANN, Z., (1935), "A drag coefficient correlation", *Z. Ver. Deutsch. Ing.*, **77**, 318-320.

SNIDER, D.M., (2001), "An incompressible three-dimensional multiphase particle-in-cell model for dense particle flows", *J. Comput. Phys.*, **170**, 523-549.

SNIDER, D.M., O'ROURKE, P.J., ANDREWS, M.J., (1998), "Sediment flow in inclined vessels calculated using a multiphase particle-in-cell model for dense particle flows", *Int. J. Multiphase Flow*, **24**, 1359-1382.

SYAMLAL, M., O'BRIEN, T., (1989), "Computer simulation of bubbles in a fluidized bed", *AIChE Symp. Ser.*, **85**, 22-31.

TAGHIPOUR, F., ELLIS, N., WONG, C., (2005), "Experimental and computational study of gas-solid fluidized bed hydrodynamics", *Chem. Eng. Sci.*, **60**, 6857-6867.

WALLIS, G.B., (1969), "One Dimensional Two-phase Flow", McGraw-Hill, New York.

WANG, J., VAN DER HOEF, M., KUIPERS, J., (2009), "Why the two-fluid model fails to predict the bed expansion characteristics of Geldart A particles in gas-fluidized beds: A tentative answer", *Chem. Eng. Sci.*, **64**, 622-625.

WEN, C., YU, Y., (1966), "Mechanics of fluidization", *Chem. Eng. Prog. Symp. Ser.*, **62**, 100-111.

WILLIAMS, F., (1985), "Combustion Theory". 2nd. Benjamin/Cummings, Menlo Park, CA.

YE, M., VAN DER HOEF, M., KUIPERS, J.A.M., (2005), "From discrete particle model to a continuous model of Geldart A particles", *Chem. Eng. Res. Des.*, **83**, 833-843

